Measurement of EPA Bunch Length

S. Bartalucci and K. Hübner

1. Introduction

The bunch length in EPA was measured using intensities up to 1.7×10^{11} electrons per bunch for 4 different RF voltages. In this note the data are discussed and an attempt is made to extract information on the longitudinal impedance of EPA following the reasoning used at DCI, and a comparison with the first, preliminary measurements by L. Rivkin is presented.

Using the Q = 1 resonator model for the ring impedance, an estimate of the energy loss into the parasitic modes per turn is given and the expected change in stable phase angle is calculated for comparison with the measured change.

As a byproduct the beam intensity measured with the wide-band pick-up and the intensity measured with the help of the position monitors (MIME set-up) are compared.

2. Measurement set-up and data

The signal from the wide-band pick-up (HR.UWB)[1]) was displayed on the scope (TEKTRONIX 7104, Serial No B032060, Plug-in 7A29). Fig. 1 shows two examples. The width of the trace is due to an unstable trigger and not due to bunch oscillations. Only one bunch was in the machine. A Gaussian of the same height and FWHH fits well the signal at low intensity (Fig. 1a). At higher intensity, the signal shape changes: the flanks get steep (Fig. 1b), a phenomenon also known from other machines.

Fig. 2 shows the plot of σ_s obtained from the measured FWHH using

$$\sigma_s = 0.425 \text{ FWHH}$$

Two series of measurements were made (27.11.86 and 18.12.86), each time with all four r.f. voltages. There is no systematic difference discernible between these two series. The dashed curves are fitted by eye.

The points on the ordinate are obtained from a calculation of σ_{so} with

$$E = \gamma\, mc^2 = 500 \text{ MeV}$$

$$\alpha = 1/\gamma_t^2 = 0.0341 \qquad [2]$$

$$U_0 = 3.481 \text{ keV} \qquad [2]$$

$$J_\varepsilon = 0.92 \qquad [3]$$

The off-set between the data extrapolation and the calculated σ_{so} is obvious. It cannot be explained with the expected resolution of pick-up plus cable and scope because this is only σ_r = 0.28 ns (8.3 cm) according to G. Schneider. The offset could either be interpreted as evidence for an effective resolution $\sigma_r' > \sigma_r$, or that the calculated σ_{so} is too small by $\Delta\sigma_o/\sigma_o$. Table I gives the numerical values.

Table I, Error in resolution or calculated σ_{so} explaining offset

V	(kV)	10	20	30	40	mean
σ_r'	(cm)	15.8	17.9	14.3	12.7	15.2
$\Delta\sigma_o/\sigma_o$	(%)	6	17	14	13	13

Inspecting

$$\sigma_{so} \approx \frac{1}{\gamma_t}\,(2\,\pi\, R/J_\varepsilon \rho\, V \cos\phi_s)\cdot E^{1/2\ \ 3/2} \qquad (1)$$

it is hard to believe that one of the individual parameters could be the cause of the error, especially the values in the parenthesis which would have to be wrong by about 26%. However, it is not excluded that the cumulative errors could be so big.

Another explanation is that our intensity monitoring system (MIME) has a negative off-set because by shifting all data points to the right, curves joining smoothly the σ_{so} points could be obtained.

In order to check MIME, all photos of the bunch current versus time were intergrated with a planimeter. The number of particles per bunch was determined using 1.26 V/A as pick-up sensitivity[1]). Fig. 3 shows a plot of N_b (pick-up) versus N_b (MIME). The least-square fit indicates that MIME has rather a positive off-set relative to the PU and, on top of it, it is very small (1.9×10^9).

As a byproduct we find that N_b (pick-up) is systematically 20% less than N_b (MIME). One quarter of this turned out to be a calibration error of MIME according to S. Battisti. There is no explanation for the remaining 15%: neither the low-frequency cut-off of the pick-up (G. Schneider) nor an error in sensitivity or time base of the scope can explain it.

Comparison with 2 other plug-in units of the same type in a scope of the same type gave only differences of the order of 1%. The time base of the scope was checked with a spectrum analyser and tracking generator. The error is below a few percent.

Since it is not evident which correction should be applied, it is preferred to work with the raw data. The intensity is the one indicated by MIME without correction for the 5% it is apparently showing too much.

3. The longitudinal impedance

The strong bunch lengthening seen in Fig. 2 is used to derive information on the impedance. The impedance of most elements of EPA has been measured. Comparison shows that the impedance of the kickers[4]) dominates. The impedance can be quite well approximated by two Q = 1 superimposed resonators of 17 MHz and 635 MHz with a respective shunt impedance of R_s = 0.24 kΩ and 4.0 kΩ[5]) for 8 kicker modules. As will be seen, for us only the higher one is of importance. Our definition is $R_s = V^2/2P$.

The approach by Hofmann and Maidment [6]) describes quite well the bunch lengthening and the blow-up of the energy spread in DCI[7]), which has a bunch length close to the one in EPA.

We follow the DCI reasoning to get the impedance. Above the turbulence threshold, the bunch length is given by

$$\left(\frac{\sigma_s}{R}\right)^3 = \frac{e\,c\,N_b}{\sqrt{2}\,\pi\,R\,h\,V\cos\phi_s}\left[\left|\frac{Z}{r}\right|_c + \left(\frac{\mathrm{Im}\,Z}{r}\right)_{eff}\right] \qquad (2)$$

where

$$\left(\frac{\mathrm{Im}\,Z}{r}\right)_{eff} = \int_0^\infty \mathrm{Im}\,\frac{Z}{r}(\omega)\,h(\omega)\,d\omega \qquad (3)$$

and

$$r = \omega/\omega_0$$

with ω_0 the circular revolution frequency. The power spectrum of a Gaussian bunch is

$$h(\omega) = \frac{\sigma_s}{\sqrt{\pi}\, c} \exp\left[-(\omega\, \sigma_s/c)^2\right] \qquad (4)$$

with

$$\int_{-\infty}^{+\infty} h(\omega)\, d\omega = 1.$$

The frequency at which $|Z/r|_c$ has to be evaluated is not so clear. We interpret it as $|Z/r|_0$. Fig. 4 shows the absolute and imaginary part of Z/r for the dominant f_r = 635 MHz resonator and $h(\omega)$ for a short bunch length (σ_s = 30 cm). If f_r is much larger than the extent of $h(\omega)$, i.e. if

$$f_r > \frac{1}{\sqrt{2}\,\pi}\,\frac{c}{\sigma_s}$$

holds, then the impedance is nearly constant in the range of $h(\omega)$ implying

$$\left|\frac{Z}{r}\right| = \left(\mathrm{Im}\,\frac{Z}{r}\right)_{eff} = \left|\frac{Z}{r}\right|_0 \qquad (5)$$

where $$\left|Z/r\right|_0 = \frac{\omega_0}{\omega_r} R_s$$

is the absolute value in the limit of zero frequency. Introducing (5) into (2) suggests that the ratio

$$\sigma_s\, (V \cos \phi_s)^{1/2} / N_b^{1/3}$$

should be equal to a constant which contains $|Z/r|_0^{1/3}$ as factor. Fig. 5 shows the data plotted accordingly. It seems that this ratio becomes indeed a constant at high intensities. This constant given by the slope of the dashed line in Fig. 5 yields the impedance

$$|Z/r|_0 = 14\ \Omega$$

or in terms of shunt impedance R_s = 3.6 kΩ.

At low intensity, the points deviate from the straight line because turbulence has ceased. The model[6]) also predicts a blow-up of energy spread, which is indeed seen in DCI. Unfortunately, we have not yet the synchrotron radiation monitoring at $D_x \neq 0$, so this valuable information, providing an additional check, was not available to us.

Note that the 17 MHz resonator is neglected because its R_s is small and it overlaps very little with $h(\omega)$.

We now check our model accordig to the reasoning developed at SPEAR[8]): It is claimed that in the turbulent regime

$$\sigma_s \approx \left(\frac{N_b}{Q_{so}^2} \right)^{1/(2+a)} \qquad (6)$$

if $\quad |Z(\omega)| \approx \omega^a .$

Q_{so} is the zero-intensity sychrotron tune. Fig. 6 shows a log-log plot of our data which seem to converge towards a straight line as supposed in (6). This straight line corresponds to a = 1.1 but the data would also be compatible with lines having a in the range from 1.0 to 1.3.

This implies $|Z/r| \approx \omega^0$ to $\omega^{0.3}$ which is compatible with our resonator model (cf. Fig. 4) having hardly any frequency dependence in the range of interest.

Since (2) is identical to (6) in our case, Fig. 5 and 6 show more or less the same thing: the first is the DCI presentation, the second the SPEAR one.

J.P. Delahaye proposed a further check, Below turbulence, where only the potential well changes, the following equation [6]) should be verified by the low-intensity data

$$\sigma^2 = \sigma_{so}^2 + \left(\frac{e\, c\, R^2}{\sqrt{2\pi}\, h} \right) \left(\frac{\mathrm{Im}\, Z}{r} \right)_{\mathrm{eff}} \left(\frac{N_b}{V \cos \phi_s\, \sigma_s} \right) \qquad (7)$$

At high intensity, above turbulence, equation (2) is used in the form

$$\sigma^2 = \left(\frac{e\, c\, R^2}{\sqrt{2\pi}\, h} \right) \left[\left| \frac{Z}{r} \right| + \left(\frac{\mathrm{Im}\, Z}{r} \right)_{\mathrm{eff}} \right] \left(\frac{N_b}{\cos \phi_s\, \sigma_s} \right) \qquad (8)$$

Equations (7) and (8) imply that the data should be on two different lines in a plot σ_s^2 versus $N_b/(V \cos \phi_s\, \sigma_s)$ depending on the intensity. The low-intensity line is indeed seen quite well whereas the line given by (8) is hardly discernible in this plot shown in Fig. 7. Using (7) $|Z/r|_0 = 16\ \Omega$ is estimated from the 10 kV data; the line through the 40 kV data gives 19 Ω; the 30 kV data give an intermediate value. Is this variation a hint that the effective Q is larger than one?

4. Bunch length from BBI

Taking the impedance R_s = 3.6 kΩ for the 635 MHz, Q = 1 resonator, σ_s can be calculated from (2). This is done by the code BBI[9]) which uses in essence (2) but does the integral (3). The result is plotted on top of the data in Fig. 8. As expected, the agreement is not bad at high intensities where turbulence is prevailing. AT low-intensities, where the bunch is supposed to lengthen due to potential well deformation, the deviations are larger, partly because the BBI calculations were made using the same ring parameters as for the calculation of σ_{so} (cf. point 2). The dashed line marks the threshold
for turbulence assuming $|Z/r| = (\mathrm{Im}\ Z/r)_{eff}$.

5. Comparison with earlier data

Earlier data [5]) are plotted in Fig. 9 and 10 with our data. Shown are also BBI calculations by L. Rivkin for $|Z/r|_0$ = 15 Ω and 7.5 Ω. Our data deviate appreciably from the old data at 10 kV, the deviation is less at 30kV. As expected, at high intensity, our data are between the two BBI predictions.

6. Estimate of parasitic losses

The ring impedance makes the particles lose energy U_{pm} per turn into parasitic modes in addition to the synchrotron radiation loss U_0.

Calculating first the loss factor

$$k_{pm}(\sigma_s) = \frac{1}{\pi}\int_0^\infty \mathrm{Re}\ Z(\omega)\ \exp\left(-\frac{\omega^2\sigma_s^2}{c^2}\right)d\omega \qquad (9)$$

from our resonator impedance for a few σ_s values and plotting it versus σ_s yields Fig. 11. A good approximation is

$$k_{pm}\ (\mathrm{V/pC}) = 1.35 \times 10^3\ \sigma_s^{-3.11}\ (\mathrm{cm}) \qquad (10)$$

exhibiting a surprisingly strong σ_s dependence.

As a check we look back at an old estimte of k_{pm} due to the kickers by A. Krusche [10]). For σ_s = 30 cm, the k_{pm} derived from the "frequency measurement" was 40 V/nC; from the "pulse technique" it was 120 V/nC; formula (10) gives 34 V/nC showing that our order of magnitude is correct.

In order to get all the parasitic losses we must not forget the loss into the high-Q resonances seen by the beam. We consider only the r.f. cavity because very few resonances were identified in other boxes as valves, electrostatic septum etc.

Table II gives the lowest eight monopole modes of a model cavity with a geometry very close to the final one.

Table II, Monopole modes of cavity (Susini II)

ℓ	f (MHz)	$R_s T^2/Q$ (Ω)
0	19	34,8
1	98	1,28
2	202	1,19
3	270	9,19
4	322	1,72
5	405	0,80
6	469	6,83
7	493	2,88
8	520	0,90

These modes were calculated with URMEL [11]. A previous comparison between SUPERFISH and URMEL had given good agreement [12]. Using

$$k_{pm} = \sum_{\ell=1}^{8} \frac{\omega_\ell}{2} \left(\frac{R_s T^2}{Q}\right)_\ell e^{-\omega_\ell^2 c^2/\sigma_s^2} \qquad (11)$$

yields Table III. Eight modes are sufficient in the sum (11) for a precision better than 1% in k_{pm} for our long bunches.

Table III, r.f. cavity loss factors versus σ_s

σ_s (cm)	20	30	60	100
k_0 (V/pC)	2.06	2.04	1.96	1.77
k_{pm}(V/pC)	3.50	0.89	0.089	0.006

The loss factor k_0 for the fundamental is shown for completeness. Since the losses into fundamental are compensated by the AVC of the cavity and do not change ϕ_s, the sum (11) starts with ℓ=1. It is obvious from Fig. 11 that k_{pm} (cavity) can be neglected.

Since $$U_{pm}(N_b) = k_{pm}(\sigma_s(N_b))e\,N_b \qquad (12)$$

holds, U_{pm} can be calculated using the measured set $\sigma_s = \sigma_s(N_b)$ from Fig. 2 and k_{pm} from (10). The result is plotted in Fig. 12 for short and long bunches.

Even at its maximum (0.22 kV) U_{pm} is much smaller than $U_0 = 3.5$ kV. For curiosity, note that we quoted $U_{pm} < 0.07$ kV in the design report for $N_b = 2.5 \times 10^{10}$, a factor 2.3 too small.

Fig. 13 gives the calculated stable phase angle

$$\phi_s = \arcsin \frac{U_0 + U_{pm}}{V} \qquad (13)$$

versus intensity for 40 kV. For 10 kV, the change is also only 0.3°. The measured change (Fig. 14) is an order of magnitude larger, which is likely due to the amplitude dependence of the phase comparator according to R. Garoby.

7. Conclusions and recommendations

Strong bunch lengthening occurs in EPA. The data are compatible with the resonator model ($Q = 1$, $f_r = 0.64$ GHz) by L. Rivkin if a shunt impedance of 3.6 kΩ is assumed implying

$$\left|Z/n\right|_0 = 14\ \Omega.$$

L. Rivkin inferred $R_s = 4$ kΩ from the impedance measurements by A. Krusche and about 2 kΩ from his bunch length measurements. The analysis is based on the combined potential well and turbulence model, which fits quite well the data at higher intensity; at low intensity, the model is less good. There is an unexplained 10% off-set between calculated and measured bunch length, which unfortunately overshadows our analysis.

The loss factor k_{pm} found from the resonator model scales like σ_s^{-3} which is a surprisingly strong dependence on σ_s. The calculated loss per turn is more than an order of magnitude smaller than the radiation loss per turn, and the estimated change of the stable phase angle is around 0.3° which is too small to be measured with the equipment at hand.

Recommendations

- remeasure $\sigma_s = \sigma_s (N_b)$ after installation of kicker complement: the impedance should increase by 3/2, any additional factor is due to the new clearing electrodes;

- observe simultaneously the frequency spectrum to see the onset of turbulence, and carefully measure Qs:

- have the intensity monitor (MIME) recalibrated;

- get the better calibrated (but apparently very elusive) current transformer;

- get the fast photo diode operational:

- get synchrotron light from $D_x \neq 0$ to the monitor in order to see the blow-up of energy spread:

- consider checking the response of the wide-band pick-up with the installed cable plus scope.

Acknowledgements

We thank for help from S. Battisti, who checked the MIME calibration, and from G. Schneider and J.F. Bottollier, who helped to check the scope calibrations. We had interesting and useful discussions with J.P. Delahaye, H. Henke, A. Hofmann and B. Zotter.

References

1) G. Schneider, Forthcoming Paper at 1987 Part. Accel. Conf. in Washington.

2) S. Bartalucci, PS/LPI Note 86-31.

3) M. Bell and H. Kugler, PS/LPI Note 86-01.

4) A. Krusche, Plot of Z/r versus f of an EPA kicker module, Priv. Comm. (26.8.1985).

5) L. Rivkin, PS-LEP Meeting (21.10.1986) and draft note "Collective effects in EPA", October 1986.

6) A. Hofmann and J. Maidment, LEP note 168 (1979).

7) J.C. Denard, J. Le Duff, M.P, Level, P.C. Marin, E.M. Sommer, H. Zyngier, IEEE Trans. Sci. NS-28 (1981) 2474.

8) A. Chao and J. Gareyte, note SPEAR-197 (1976): P.B. Wilson et al., IEEE Trans. Nucl. Sci. NS-24 (1977) 1211 (We interpret their Z as $|Z|$.)

9) M. Gygi-Hanney, A. Hofmann, K. Hübner. B. Zotter, report CERN/LEP-TH/83-2.

10) A. Krusche, priv. comm. (14.1.1985).

11) M. Bell, URMEL results July 1984.

12) M. Bell and W. Pirkl, PS/DL/LPI Note 84-22.

Figure Captions

Fig. 1 Excample of bunches. The crosses pertain to a Gaussian of same height and FWHH. a) $N_b = 2.10^9$, 1 ns/Div; b) $N_b = 1.7.10^{11}$, 2 ns/Div.

Fig. 2 Measured σ_s versus bunch intensity. Dashed curves fitted by eye.

Fig. 3 N_b (Wide-band pick-up) versus N_b (MIME). The dashed straight line (N_b (PU) = 0.80 N_b (MIME) - $0.16.10^{10}$) is a fit to all data points.

Fig. 4 Normalized Im (Z/r) and $|Z/r|$ versus f/fr for a Q = 1 resonator at 635 MHz. The bunch spectrum h is drawn for σ_s = 30 cm.

Fig. 5 σ_s (V cos ϕ_s) versus $N_b^{1/3}$. The straight line $|Z/r|_0$ = 13.6 Ω.

Fig. 6 N_b/Q_{so}^2 versus σ_s. The straight line is the expected behaviour for $|Z| \approx \omega^a$ with a = 1.1.

Fig. 7 σ_s^2 versus $N_b/(\sigma_s\ V \cos\phi_s)$. Straight lines fitted to 10 kV and 40 kV data by eye.

Fig. 8 $\sigma_s = \sigma_s\ (N_b)$ as calculated by BBI (full lines) for $|Z/r|_0$ = 13.6 Ω superimposed on data. Thick dashed line: turbulence threshold.

Fig. 9 $\sigma_s = \sigma_s\ (N_b)$. Dots: new data; crosses : L. Rivkin's data; Full lines: BBI results for $|Z/r|_0$ = 15 Ω and 7.5 Ω by L. Rivkin. V = 10 kV.

Fig. 10 The same as Fig. 9 but V = 30 kV.

Fig. 11 Loss factor K_{pm} versus σ_s. Crosses: calculated from resonator impedance. Cercles: calculated for r.f. cavity.

Fig. 12 Calculated loss per turn into parasitic modes versus bunch intensity.

Fig. 13 Calculated stable phase angle versus bunch intensity.

Fig. 14 Measurement of ϕ_s versus N_b with a single bunch.

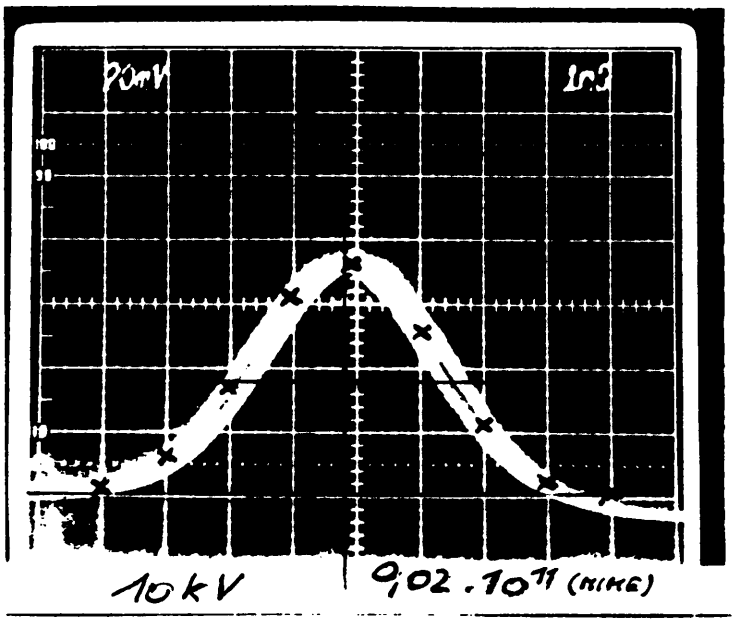

a)

1 ns / Div

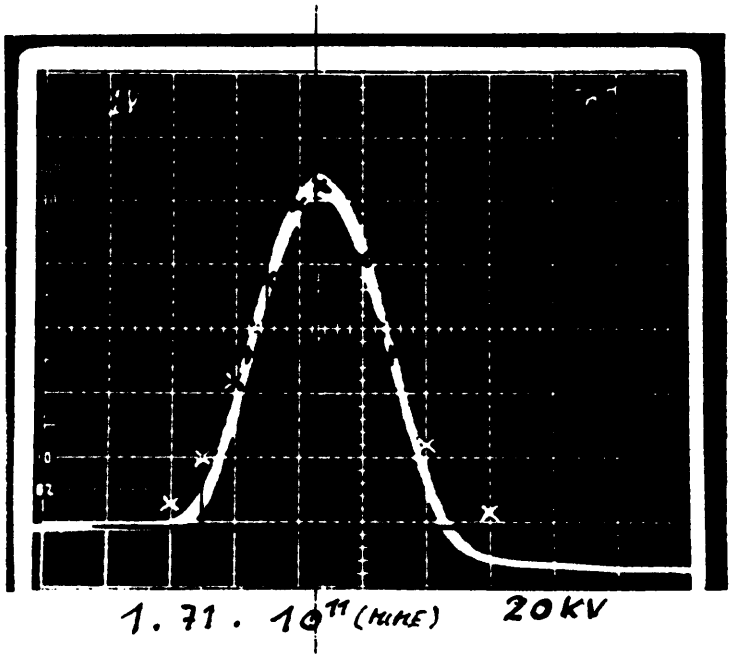

b)

2 ns / Div

Fig. 1 Signal from wide-band pick-up versus time
The crosses x pertain to a Gaussian of same height and FWHH

8.1.87

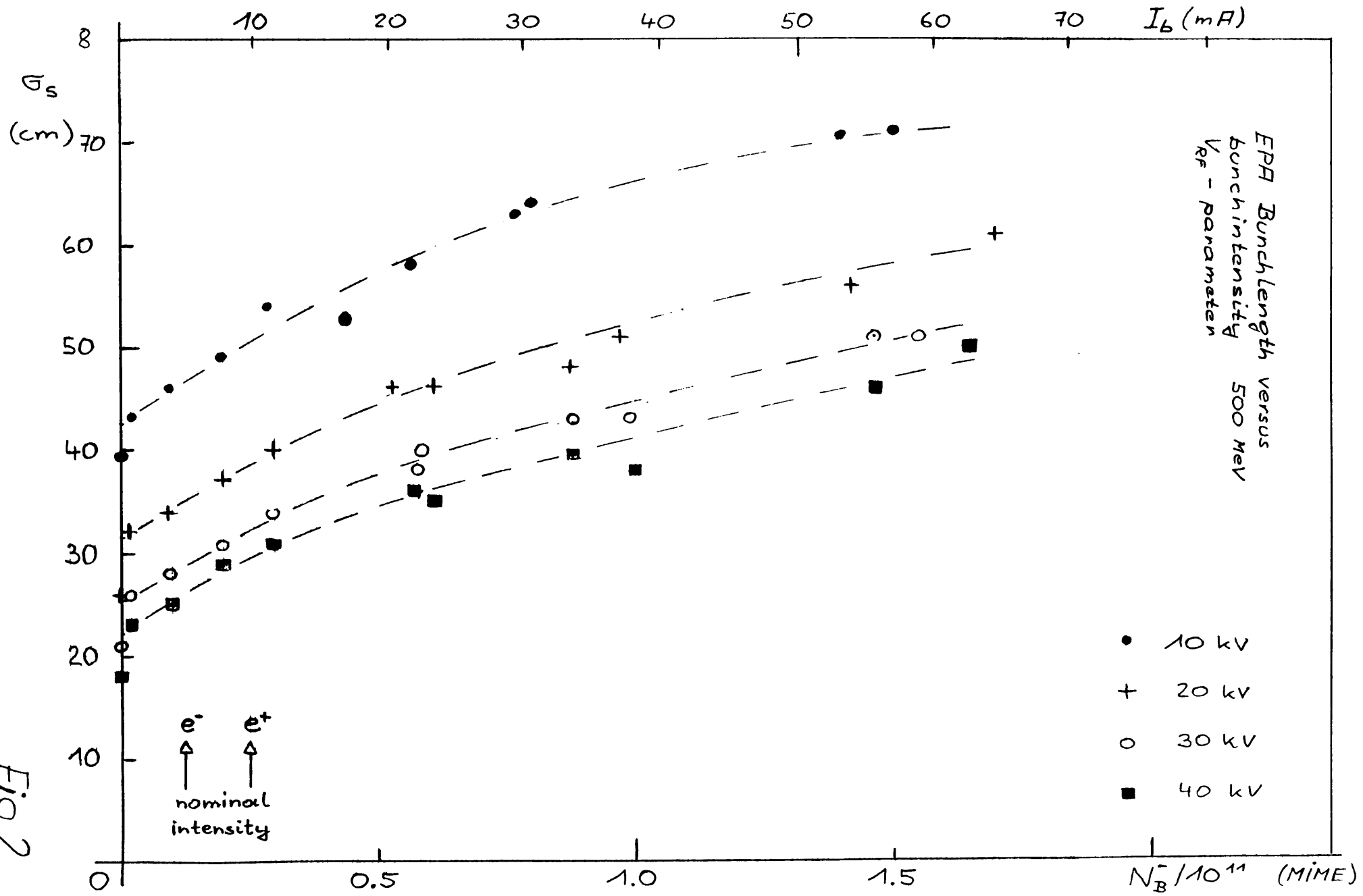
EPA Bunchlength versus
bunchintensity 500 MeV
V_{RF} - parameter
σ_s (cm)
I_b (mA)
10
20
30
40
50
60
70
8
60
50
40
30
20
10
0
0.5
1.0
1.5
$N_B^-/10^{11}$ (MIME)
10 kV
20 kV
30 kV
40 kV
e^-
e^+
nominal intensity

Fig. 2

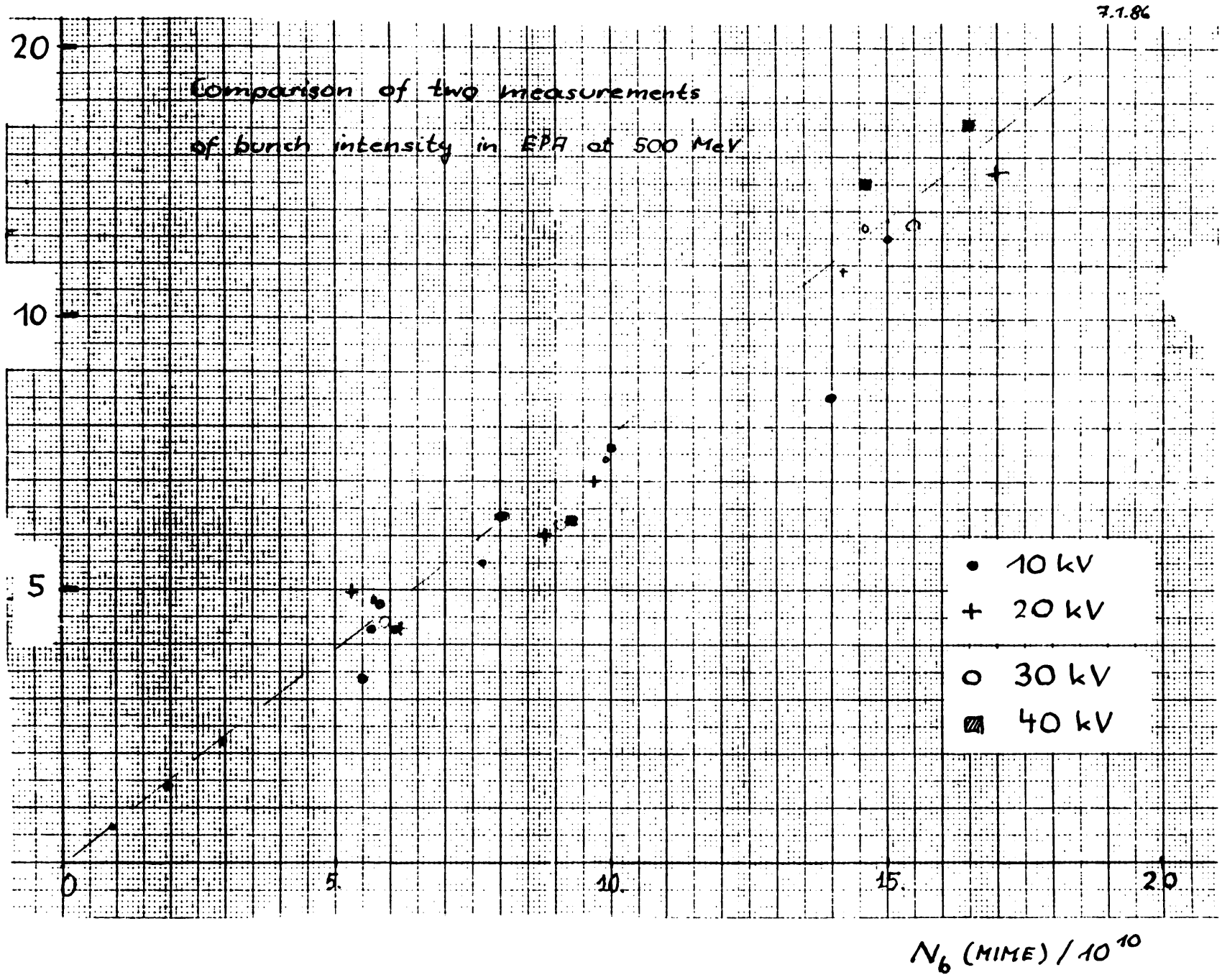
7.1.86
Comparison of two measurements
of bunch intensity in EPA at 500 MeV
$N_b / 10^{10}$
(Wide-band pick-up)
20
10
5
0
5.
10.
15.
20
N_b (MIME) / 10^{10}
• 10 kV
+ 20 kV
o 30 kV
40 kV

Fig. 3

Impedance of resonator $Q = 1$ $f_r = 0.025$ GHz

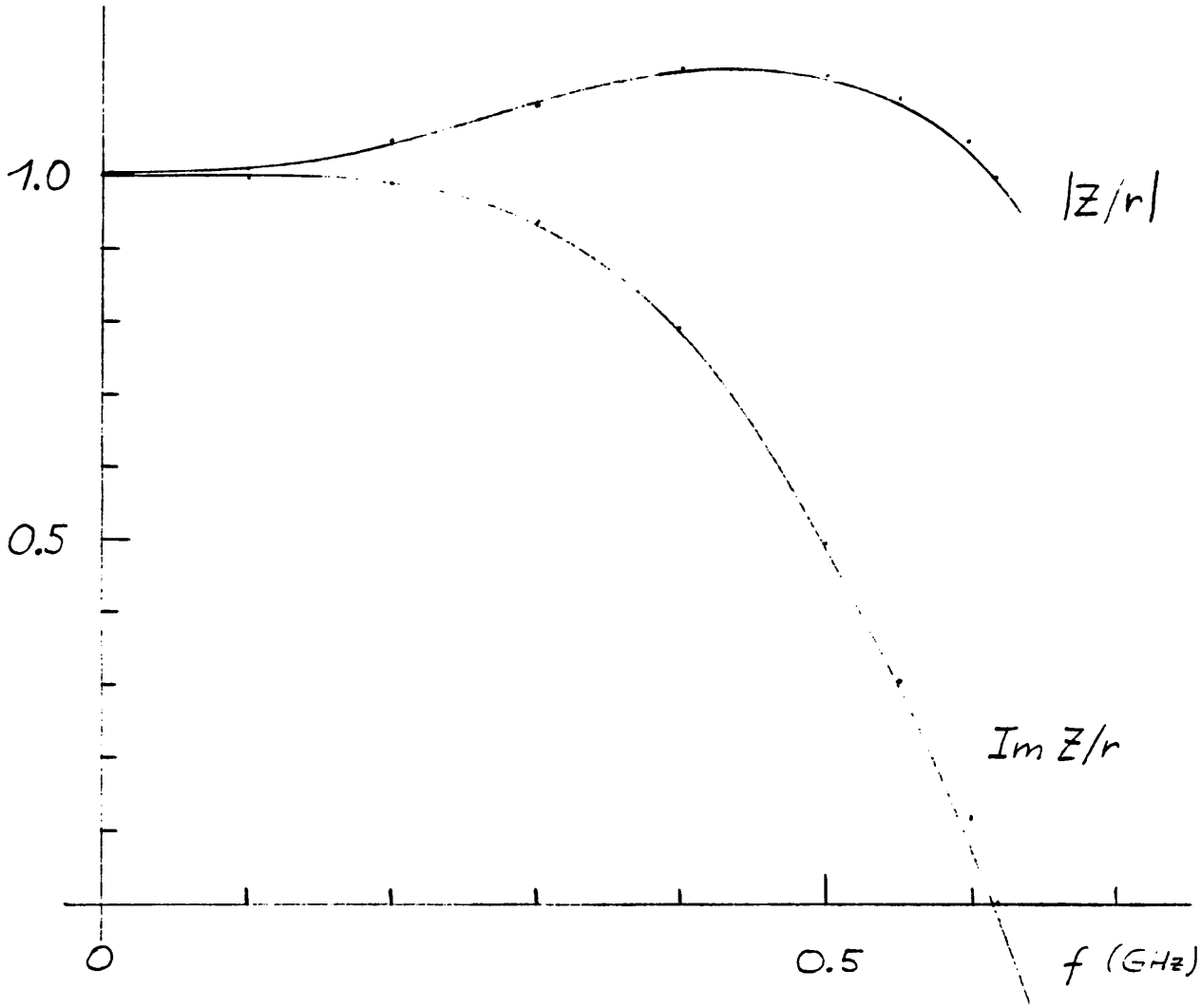

power spectrum of bunch

$\sigma_s = 30$ cm

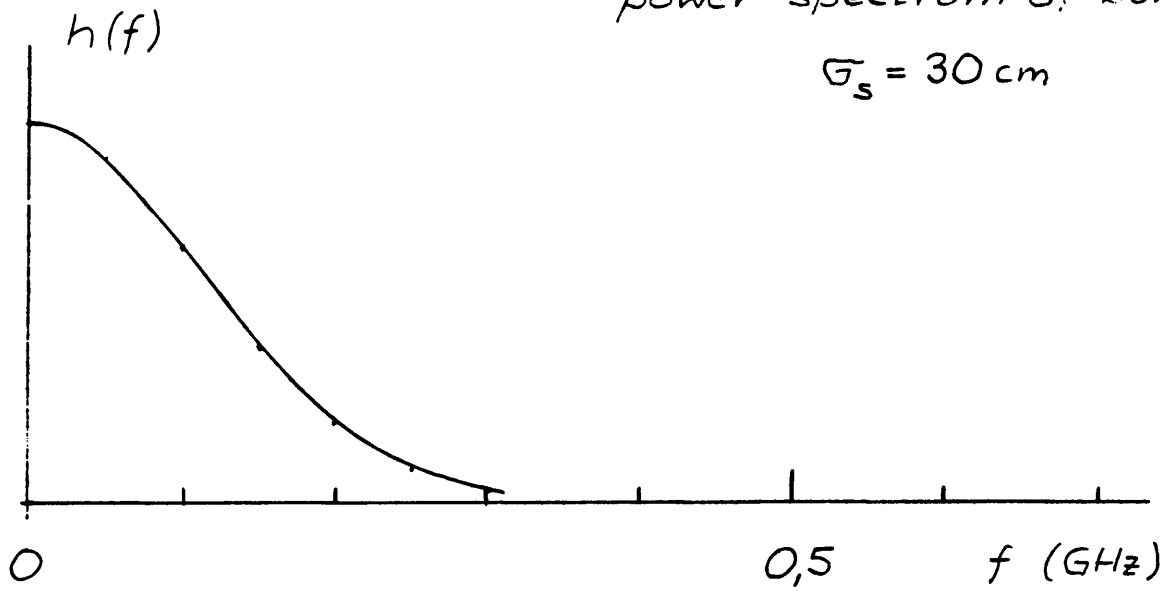

Fig. 4

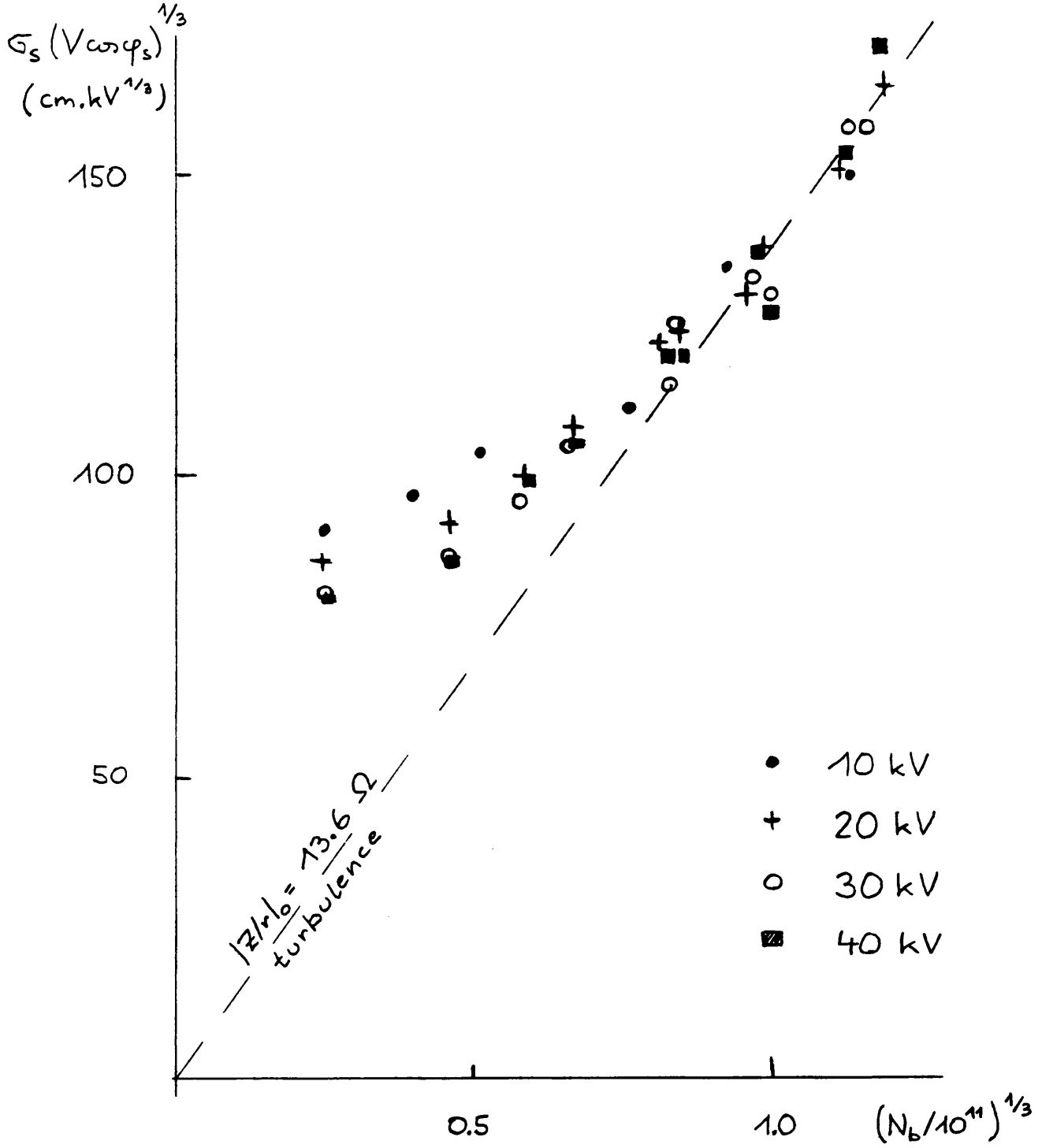
$\sigma_s (V \cos\varphi_s)^{1/3}$
(cm.kV$^{1/3}$)
150
100
50
0.5
1.0
$(N_b/10^{11})^{1/3}$
|Z/r|$_o$ = 13.6 Ω
turbulence
10 kV
20 kV
30 kV
40 kV

Fig. 5

16.1.87

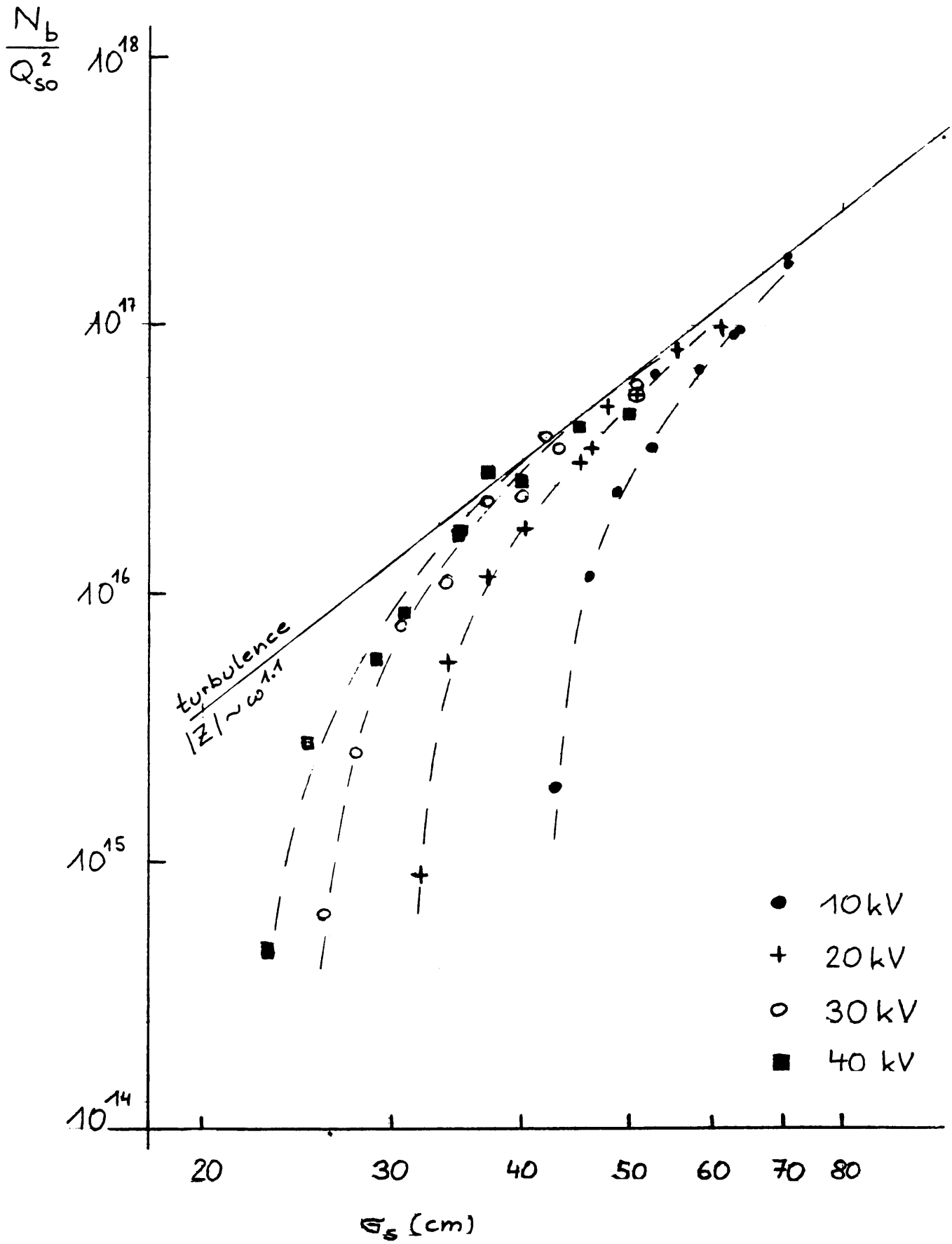
$\frac{N_b}{Q_{so}^2}$
10^{18}
10^{17}
10^{16}
10^{15}
10^{14}
turbulence
$|Z| \sim \omega^{1.1}$
10 kV
20 kV
30 kV
40 kV
20
30
40
50
60
70
80
σ_s (cm)

Fig. 6

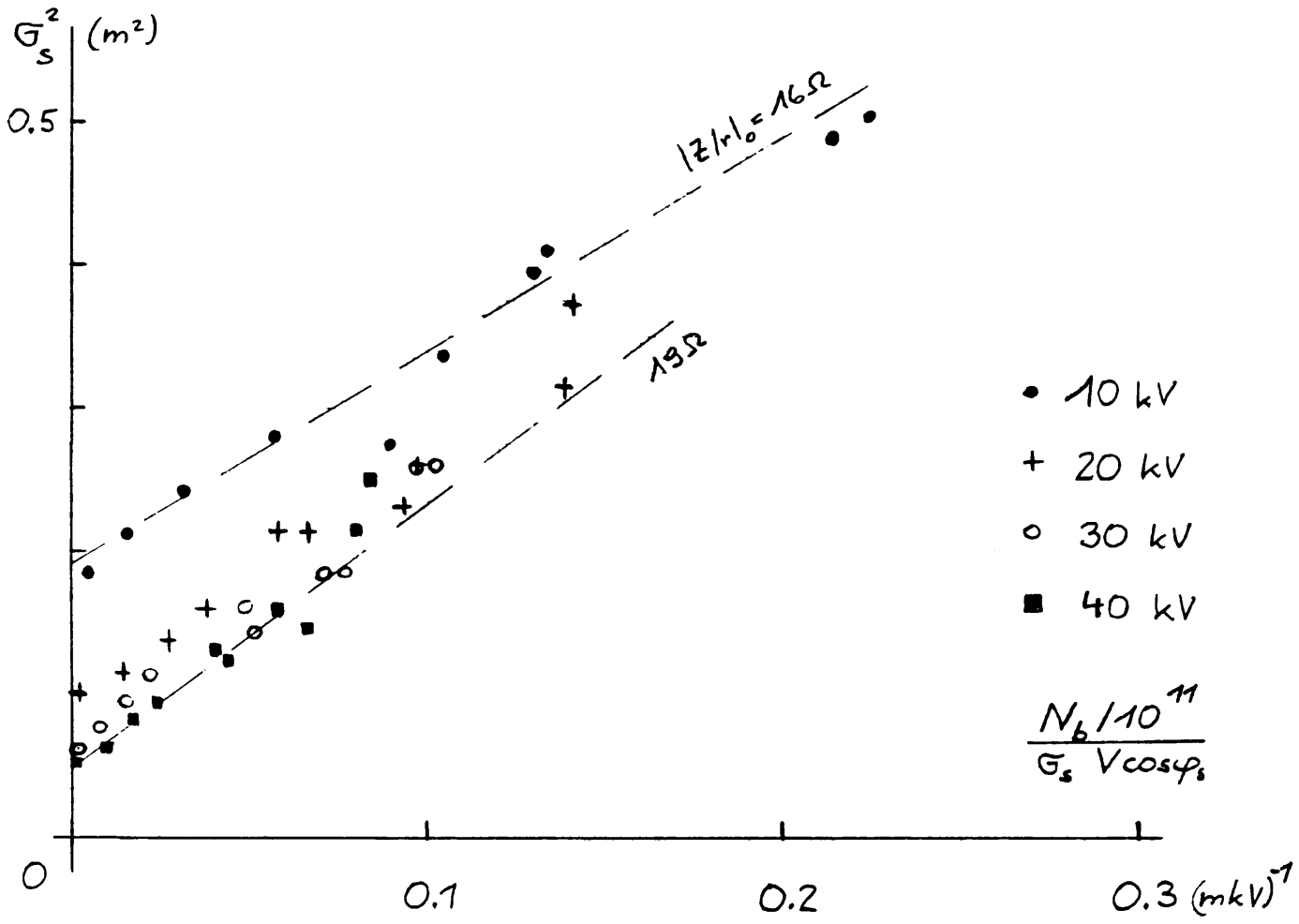
σ_s^2 (m²)
0.5
0
0.1
0.2
0.3 (mkV)⁻¹
|Z/n|₀ = 16Ω
19Ω
• 10 kV
+ 20 kV
○ 30 kV
■ 40 kV
$\frac{N_b/10^{11}}{\sigma_s V \cos\varphi_s}$

Fig. 7

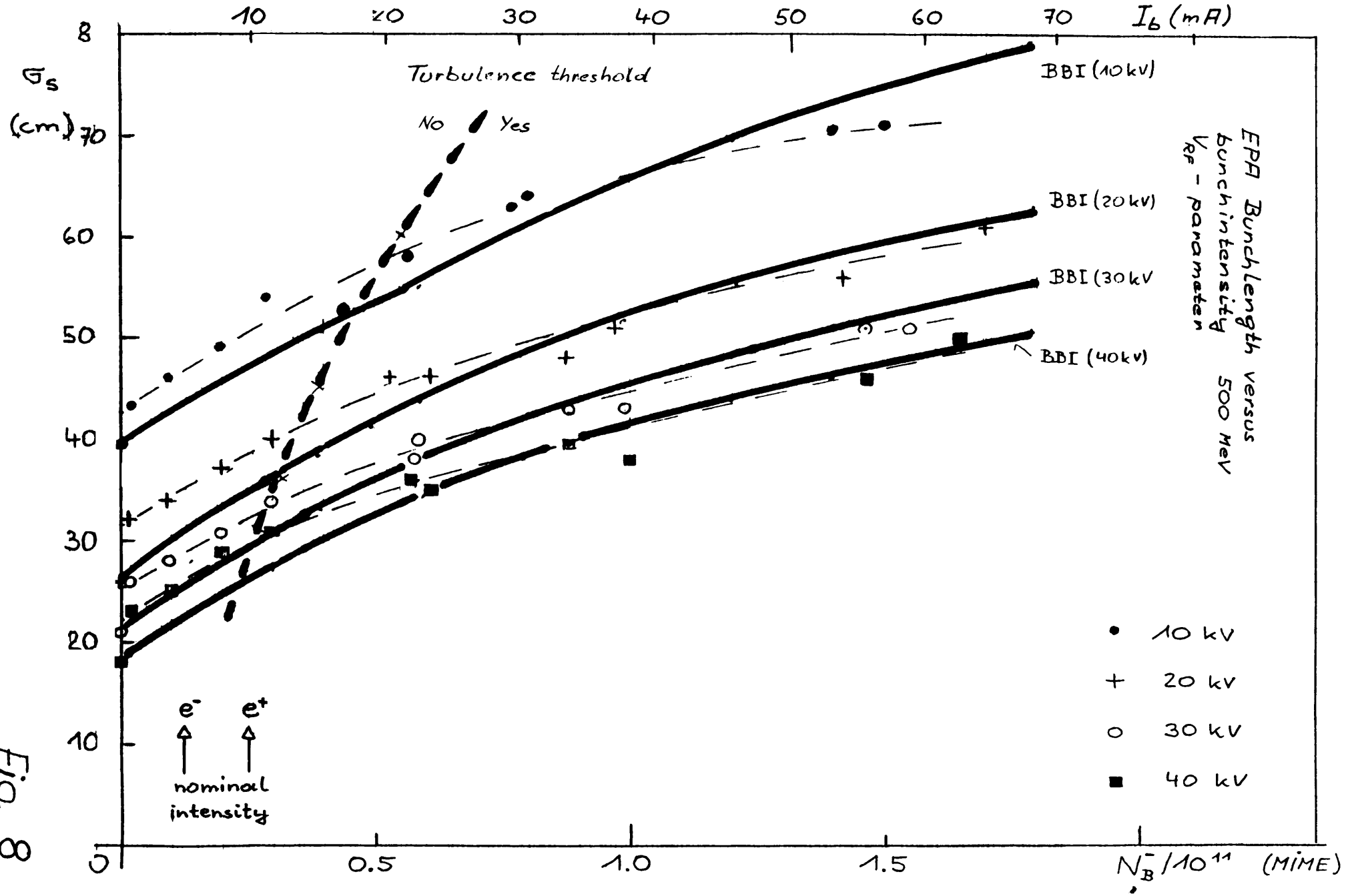
I_b (mA)
10
20
30
40
50
60
70
σ_s (cm)
8
70
60
50
40
30
20
10
0
0.5
1.0
1.5
$N_B^-/10^{11}$ (MIME)
Turbulence threshold
No
Yes
BBI (10kV)
BBI (20kV)
BBI (30kV)
BBI (40kV)
EPA Bunchlength versus bunchintensity 500 MeV
V_{RF} - parameter
10 kV
20 kV
30 kV
40 kV
e^-
e^+
nominal intensity

Fig. 8

8.1.87

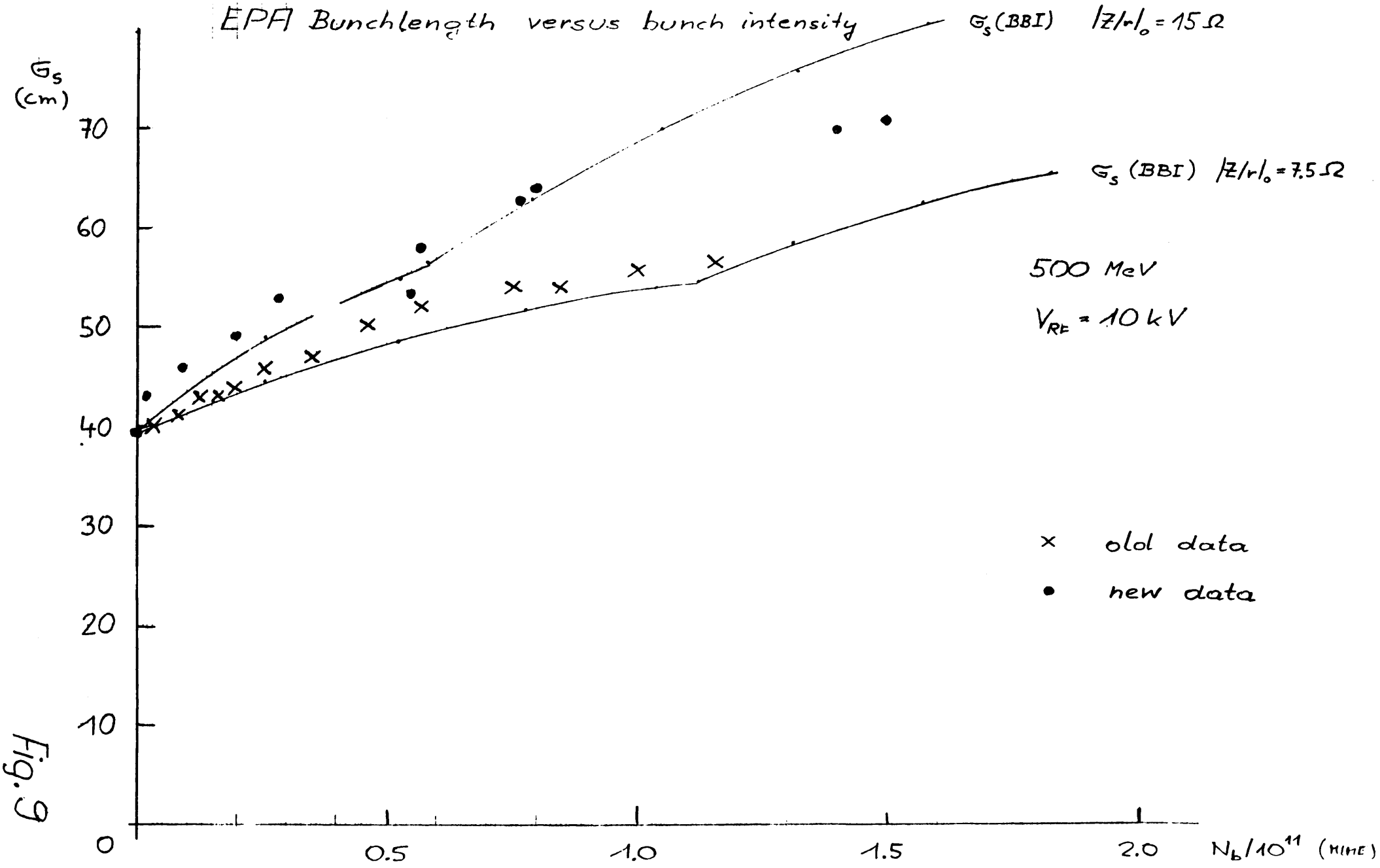
EPA Bunchlength versus bunch intensity
σ_s (BBI) $|Z/n|_0 = 15\,\Omega$
σ_s (BBI) $|Z/n|_0 = 7.5\,\Omega$
σ_s (cm)
500 MeV
V_{RF} = 10 kV
× old data
• new data
0
10
20
30
40
50
60
70
0.5
1.0
1.5
2.0
$N_b/10^{11}$ (MINE)

Fig. 9

9.1.87

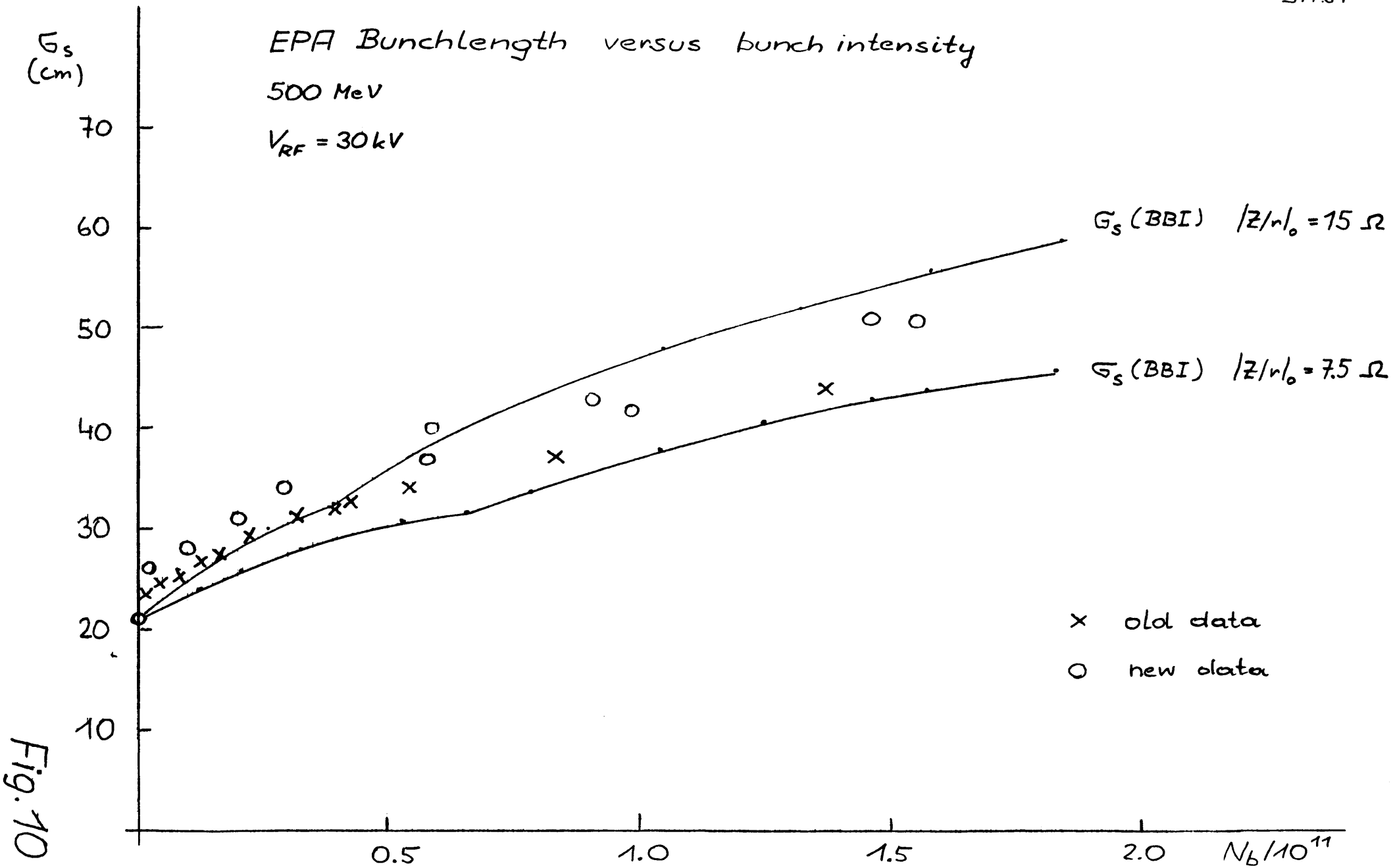
EPA Bunchlength versus bunch intensity
500 MeV
V_{RF} = 30 kV
σ_s (cm)
70
60
50
40
30
20
10
0.5
1.0
1.5
2.0
$N_b/10^{11}$
σ_s (BBI) $|Z/n|_0$ = 15 Ω
σ_s (BBI) $|Z/n|_0$ = 7.5 Ω
× old data
○ new data

Fig. 10

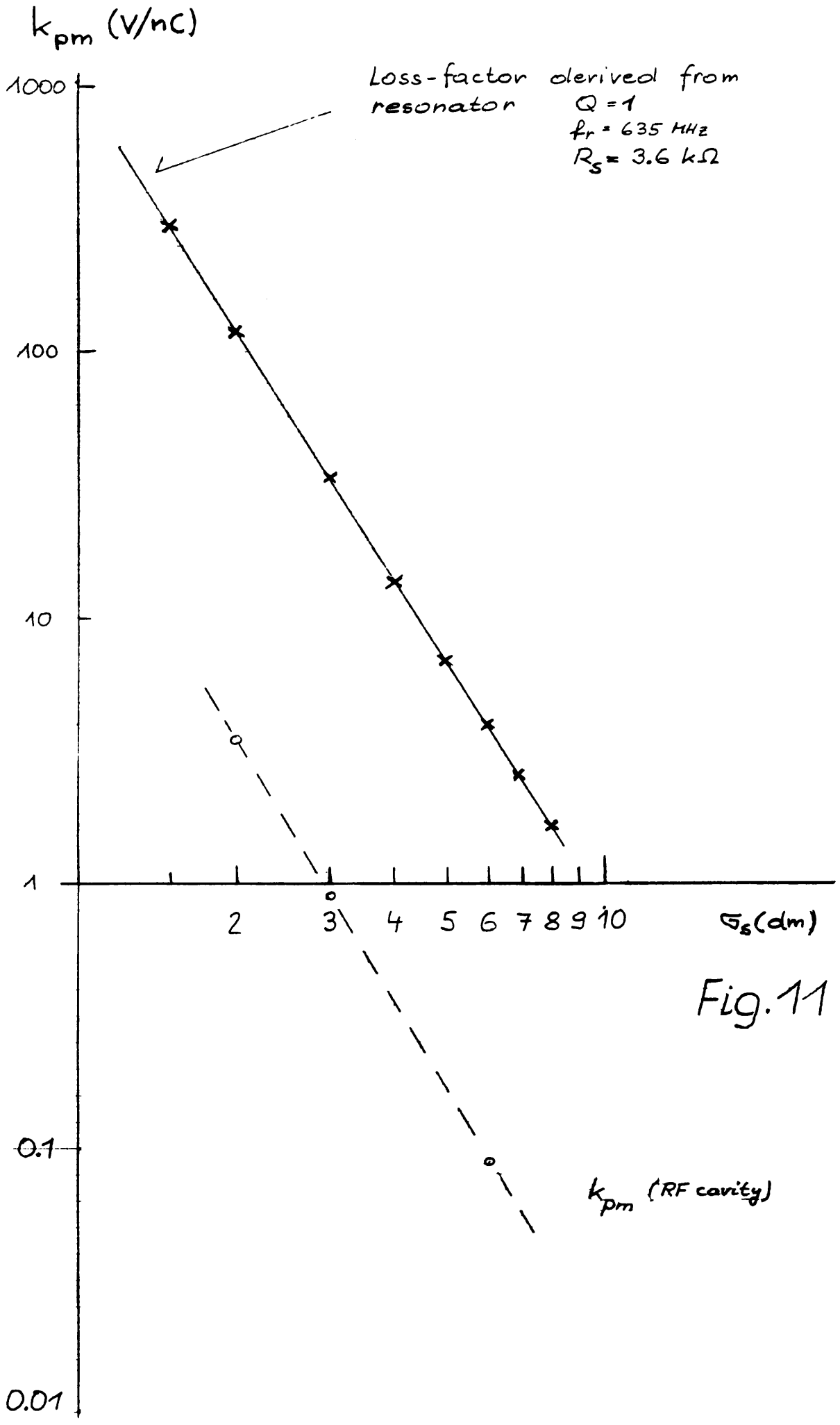
k_{pm} (V/nC)
1000
100
10
1
0.1
0.01
Loss-factor oleriveol from resonator Q = 1
f_r = 635 MHz
R_s = 3.6 kΩ
2
3
4
5
6
7
8
9
10
σ_s(dm)
k_{pm} (RF cavity)

Fig. 11

Expected parasitic energy loss per turn

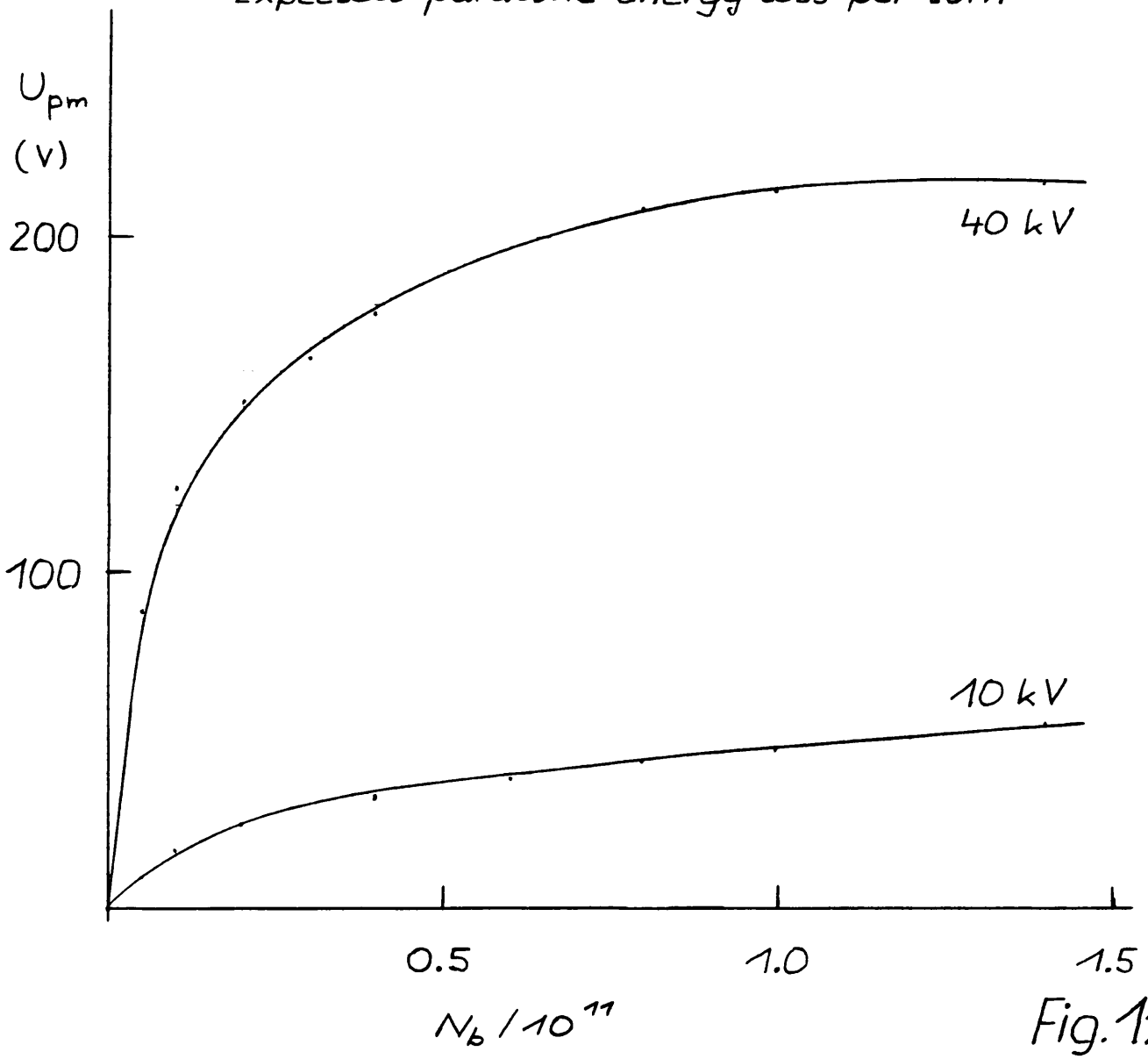

Fig. 12

$180° - \varphi_s$ Expected variation of stable phase angle

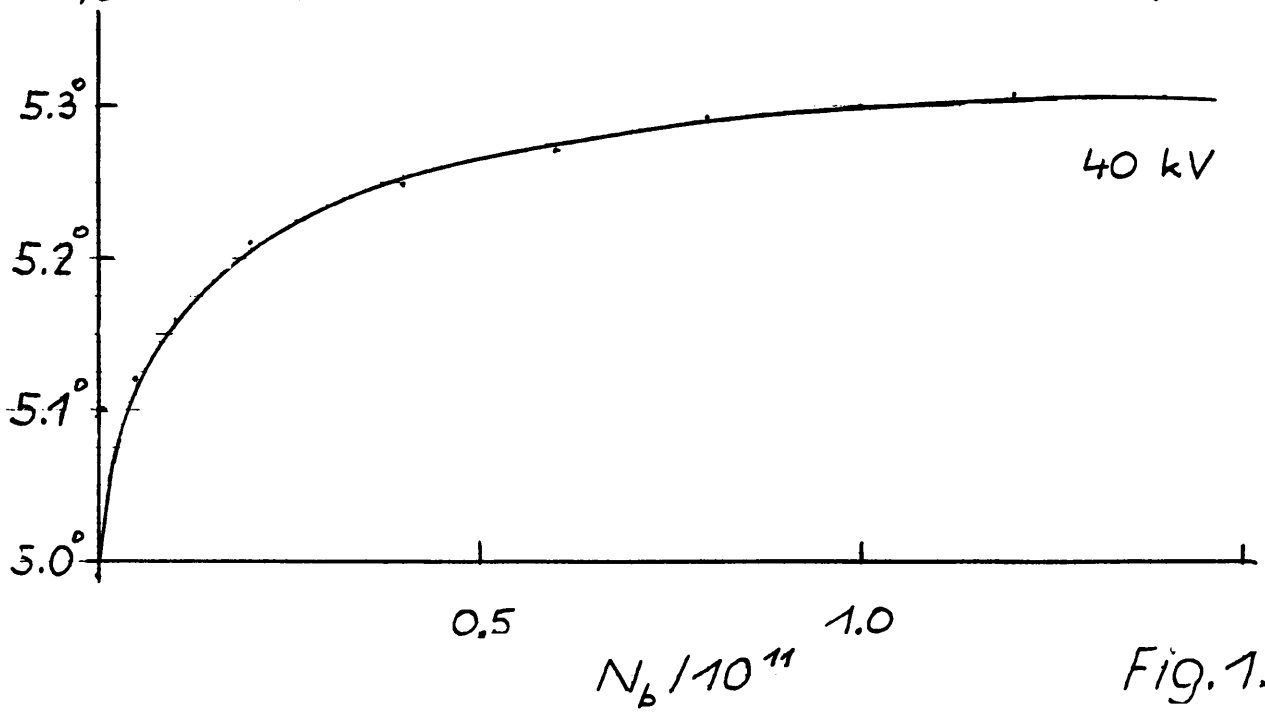

Fig. 13

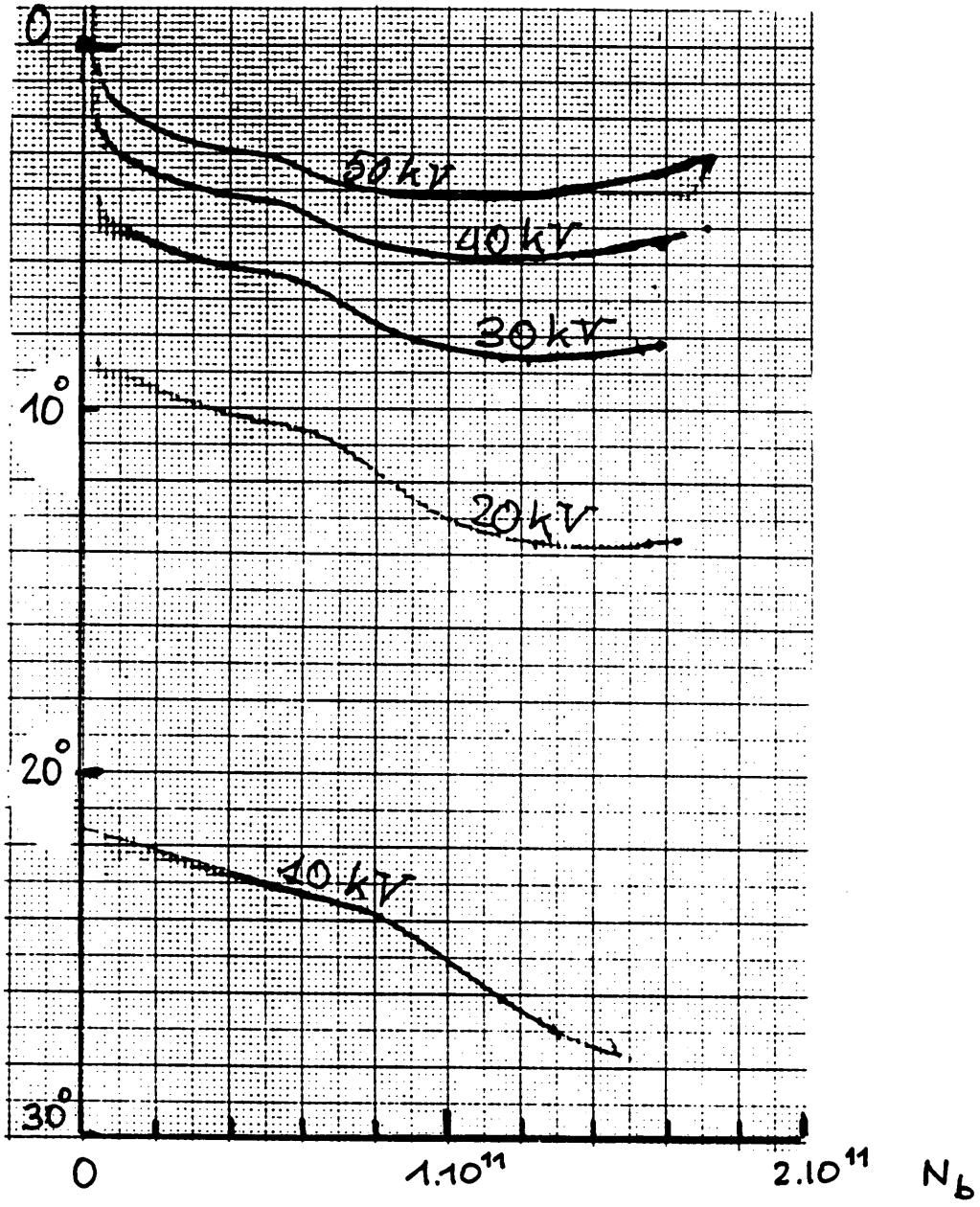

Fig. 14 Measurement of φ_s versus N_b
Single bunch.

Y. Baconnier
S. Bartalucci
S. Battisti
M. Bell
D. Blechschmidt
J.F. Bottolier
E. Brouzet
J. Broere
R. Cappi
J.P. Delahaye
F. Di Maio
B. Frammery
R. Garoby
A. Hofmann
H. Kugler
A. Krusche
A. Lévy-Mandel
J.H.B. Madsen
G. Nassibian
F. Pedersen
F. Perriollat
A. Poncet
J.P. Potier
A. Riche
J.P. Riunaud
A. Susini
D. Warner
B. Zotter